ISSN: 2424-8460(O)
2251-2608(P)

Original Research Article

A method of data supplementing Global PBL SO_2 based on OMI

Chongyang Kang[1], Xiaofang Yang [1], Zhuoying He[1], Kedi Mi[2], Jie Hu[2], Xiaorong Yu[2]

1 Department of Education, Sichuan Tecnology and Business University, Meishan, Sichuan, 620000, China
2 Department of Library, Sichuan Tecnology and Business University , Meishan, Sichuan, 620000, China

Abstract: Sulfur dioxide(SO_2) is an important pollutant gas that affects environment of our lives. Although we had made lots of detections, but still can not receive the distribution of SO_2 in the world. Compared with great success in UV-vis spectrometers from remote sensing in OMI and OMPS, can provide SO_2 data in a huge range and daily, but cannot receive data as there is no sunshine, this is difficult for researchers to do their study in global or area in high latitudes. In this paper, we tried to supplement the PBL SO_2 in the whole world, based on the data of OMISO_2, by the function derivative algorithm to segment approximation, and verified the method in the area, where OMI SO_2 data are complete. The results show that the spatial distribution of SO_2 in the global atmospheric boundary layer is obviously latitudinal zonality. SO_2 columns and its variation trend are the same or similar in the same latitude during the year. Through verification we found that the partition below 5° latitude seldom affect the estimation, The accuracy is good in the region where there is no SO_2 columns mutation, more than 90% of the grids which differences between the estimation and the truth are in a range of [-0.2DU, 0.2DU], less than the multi-day OMI monthly error of 0.2DU, the function is suitable in this situation, and the estimation will be biased in the region where the volcanic eruption, causes the monthly average SO_2 columns mutation, but choosing data from the month nearby with no volcanic eruption can helps to eliminate the effects of volcanic eruptions and also can estimate the areas affected by volcanic eruptions.

Keywords: PBL SO_2; OMI; The function derivative; Verification; SO_2 column

1. Introduction

Sulfur dioxide (SO_2) is an important pollutant gas that significant impacts on the environment and climate at global, regional and scales[1], mainly come from man-made and natural emissions[2-4]. And it is secondary pollutants influence far beyond itself, dry fall form of sulfate aerosols is the main element of haze, reduce atmospheric visibility and solar radiation, influence the formation of clouds and atmospheric circulation; wet deposition causes, acid rain and damages the buildings and vegetation environment in the acid rain and damages the buildings and acid rain and damages the buildings and vegetation environment in the area .Photochemical reaction to form sulfuric acid mist, directly endanger body health of humans, and even endanger our lives, the 1952 London smog event led to the deaths more than 8000 people, become one of the eight major public nuisance incidents in the 20th century[5]. According to studies about the correlations between SO_2 and diseases, the concentration of SO_2 in the atmosphere is highly correlated with lung cancer and AMI mortality[6-8].

The priority traditional monitoring methods are chemical, electrochemical and foundation of optical method, all are based on the point monitoring, with a complex operation, highly cost on equipment maintenance, can not conducive to large area SO_2 monitoring spatial distribution and changes. In 1983, Krueger became the first senior that found SO_2 from EI Chichon volcanic eruption by remote sensing satellite of Total Ozone Mapping Spectrometer (TOMS), which is onboard NASA's Nimbus satellite, became the first man opens the door to monitor gas by remote sensing. In 1995, anthropogenic SO_2 emission was found by Global Ozone Monitoring

Experiment (GOME) ; In nearly 20 years later, the development and utilization of ultraviolet spectrum fitting technology, promote the wide use of it on atmospheric remote sensing monitoring, such as the Scanning Imaging Absorption Spectrometer for Atmospheric CHartographY (SCIAMACHY), carried on ENVISAT satellite[9], Global Ozone Monitoring Experiment-2 (GOME-2) on the MetOp - A satellite [4]; The most applications are the Ozone Monitoring Instrument(OMI)[10]on NASA's Aura spacecraft in 2004 and the Ozone Mapping and Profiler Suite (OMPS)[11]on board of the NASA-NOAA Suomi National Polar-orbiting Partnership (SNPP) in 2011, which are high spectral sensors, can provide high resolution and daily global atmospheric boundary data of SO_2 vertical value.

Scholars have done lots of researches on detection of SO_2 in the atmosphere by remote sensing. Early detection mainly concentrated on SO_2 emission in the volcanic eruption, Carn measured SO_2 emissions during each of Nyamuragira's 13 most recent eruptions by TOMS from 1978 to 2002 [12]. Khokhar investigates the systematic bias in instrumental effects of GOME and does a quantitative study about 20 volcanoes from Italy, Iceland, Congo/Zaire, Ecuador, Japan, Vanuatu Island and, Mexico between 1996 to 2002 by GOME[13] .In recent years, the emission of SO_2 comes from humans is widely monitoring by remote sensing. Michael Eisinger does a study about Nyamuragira volcano and Popocatepetl volcano in December 1996, also to anthropogenic pollution event over the Balkans on 8 February 1998[14]. In the global region, Fioletov obtained the global large SO_2 emission sources through the OMI data[15], Zhang Yan conducted a long series comparison of the data between OMI and OMPS, from 2012-2015 in the global range[1]; Krotkov compared the pollution changes of SO_2 and NO_2 in the global regions from 2005 to 2015 by OMI data[16]. In local monitoring, Jiang Jie tested the SO_2 concentration in China based on the OMI data and estimated the emissions[17]. D Xue analyzed estimation of daily average surface SO_2 concentration by OMISO2 of Shanghai from 2004 to 2012[18]. Zhao Jun studied the distribution of SO_2 in Lanzhou and surrounding areas by using OMI data[19]. A study by Kang Chongyang shows that summer monsoon has a significant effect on the reduction of SO_2 in the monsoon region of China, and the SO_2 concentration is only affected by winter monsoon in the non-monsoon area[20]. Influenced by the rotation and the revolution of the earth, the satellite cannot receive the radiation of the sun at high latitudes and can not collect data, especially in the middle and high latitudes. Although do lots of measured by researchers all over the world about the concentration of SO_2 in the atmosphere, but still there was no general image received about the global distribution of SO_2 concentration[21].

In this study, we use the daily products of OMI SO_2 L2 V003 in 2014, with the ordinary kriging interpolation allocate to grid cells of 0.125 °×0.125 ° in latitude and longitude, get monthly average SO_2 in global, try to complement the missing data in the global by a mathematical method based on OMI SO_2, complete the annual global PBL SO_2's spatial distribution, and verify the accuracy of the method in regions of 50 ° ~ 53 ° N and 45 ° N ~ 55 ° N.

2. Data sources and methods

2.1. Data sources

Ozone Monitoring Instrument (OMI) is a wide-angle, non-scanning, nadir-viewing near-UV /Visible CCD spectrometer aboard NASA's Earth Observing System (EOS) Aura satellite, launched on July 15, 2004, and collected data since August 9,2004(Levelt et al., 2006a; Schoeberl et al.,2006). It is one of NASA's three-platform Earth Observing System (EOS), mainly mission is studying the chemistry and dynamics of Earth's atmosphere,

from ground through the mesosphere, can monitor distribution and changing of SO_2 both come from nature and humans.

OMI, co-authored by NASA in the Netherlands and Finland, is a successor to GOME and SCIAMACHY. With an orbital scan of 2600km and a spatial resolution of 13km × 24km, and by 28 km × 150 km at swath edges, covers the globe once a day. Has three channels with wavelength coverage of 270-500 nm and an average spectral resolution of 0.5 nm. The sensor mainly monitors atmospheric ozone concentration and profile, aerosols, clouds, surface UV radiation, and other trace gases such as NO_2, SO_2, HCHO, BrO and so on. it has product level is divided into: Level 1B, Level 2, Level 2G, Level 3[10].

In this study, The OMSO2 data comes from http://mirador.gsfc.nasa.gov, can be available from NASA Goddard Earth Science (GES) and Information Service Center (DISC) publicly, which reflects the concentration of SO_2 in the atmospheric boundary layer corresponding to a height of less than 2 km and center of mass altitude(CMA) of 0.9km, contains SO_2 vertical densities (VCDs) in Dobson units (1DU = 2.69×10^{16} molecules•cm^{-2}), mainly used for studying SO_2 pollution in the near-surface atmosphere.

The inversion algorithm of OMI SO_2 has successively undergone the Linear Fit (LF)[22], Band Residual Difference algorithm (BRD)[10] and now Principal Component Analysis (PCA)[23]. BRD is sensitive to SO_2 pollution in PBL, but makes large noise and unphysical biases particularly at high latitudes; LF is more suitable to volcano, and PCA algorithm is a method of principal component analysis, based on the related results of O_3 absorption, surface reflectance, instrument noise and Ring effect measured without SO_2 pollution, combined with the SO_2 Jacobian matrix of radiation transmission simulation, directly acquire SO_2 vertical value in PBL. The standard deviation (sigma) of the instantaneous field of view is a criterion for evaluation of SO_2 extraction. The PCA algorithm is less than 0.5 DU in the equatorial Pacific without SO_2 pollution, less than half of the BRD. In the high latitudes, The sigma is between 0.7 and 0.9 DU, which is also twice as small as the BRD algorithm[23], allows smaller sources to be detected from space[10].

2.2. Data processing

Data exclude: they could be more noise far beyond the center of swath, in this study, we exclude pixels with large FOVs at the edges of swath (rows<5 or rows>54, SO_2 value<0DU); data, and data which Solar Zenith Angle (ZSA) >70 °; OMI SO_2 becomes more sensitive to clouds, we also exclude data, which Cloud Fraction>0.3,and receive data of Latitude, longitude, SO_2 values, this the first step of the processing.

Ordinary kriging Interpolation: Through previous experiments, we found that gridded at 0.125° × 0.125°, had the greatest correlation with data comes from the official.

Monthly average: The standard deviation of PCA – retrieved background SO_2 is 0.5DU and can be reduced by average, we use SO_2 monthly average in our study.

Zone processing: three characteristics of the experiment are used in global SO_2 distribution zoning, to recover missing data and verify the method in a zone where data are complemented.

Complete maps: All data will be restored on the basis of zoning, and then grid merge to complete the maps of global SO_2 spatial distribution.

2.3. Methods

Through the previous study found that the natural breakpoint method can more accurately reflect the spatial distribution of SO_2, in this paper, the amount of SO_2 is divided as shown in **Table 1**.

Table 1. The six-level division criteria about Global SO_2 value.

level	Annual average of SO_2 value
1	0 ~ 0.474DU
2	0.474DU ~ 0.616DU
3	0616DU ~ 0.793DU
4	0.793DU ~ 1.076DU
5	1.076DU ~ 1.959DU
6	1.959DU ~ 4.84DU
7	>4.84DU

Discriminate the spatial distribution of Monthly average SO_2 value in the same latitude during the Year, this is central in our study. Two methods are used to prove it, the first method is: Randomly generate a latitude line in the area where data are complete, extract the SO_2 values by the latitude line, and check the spatial distribution on this latitude. The second method is: At different latitudes of 53 ° N and 33 ° N, seven cities are selected and corresponding SO_2 values are extracted, SO_2 values of four cities in 53 ° N are the extension of interruption in January, the trend is judged and verified during the year. The results showed that the average monthly SO_2 are the same or similar on the same latitude and have the same or similar trend in the year except for the area with high emissions, although SO_2 values are influenced by many aspects.

A quadratic equation fitting. It was found that[20], SO_2 column were negatively correlated with temperature at a confidence level of $\alpha = 0.01$ in most areas, except area with highly SO_2 values, and temperature was directly related to direct declination of the sun. In this paper, we selected the region without SO_2 emission in the Atlantic Ocean (longitude 120 ° W ~ 140 ° W and latitude 40 ° S ~ 40 ° N), measured the latitude of the first-order SO_2 column along the axis of symmetry, and found that except for October to December, the latitudinal axis of the other months coincided with the corresponding solar decadal on the 15th. From October to December, the difference between Sun declination and latitude axis of symmetry in level 1is larger, resulted by area of level 2 (As shown in **Table 2**).

For regions with more data are serious missing, the fitting function cannot reflect the real changing situation only based on the data in that area. Averaged the difference between the average value of the existing data and the corresponding data in the band nearby, estimate data by the average and the nearby, then make function fitting, supply missing data by fitting function and existing ones.

Evaluation of the rationality is important. The difference between the estimated value and the actual value is made.in range of [-0.2DU, 0.2DU], the estimation seems excellent, in ranges of [-0.5DU, -0.2DU) and (0.2 DU, 0.5DU], the valuation is good and the valuation is modest at [-0.8DU, -0.5DU) and (0.5DU, 0.8DU], poor in the range of [-1.5DU, -0.8DU) and (0.8DU, 1.5DU], more than 1.5 DU or less than -1.5 DU, the valuation is extremely poor.

Calculate the latitude of the sun's direct point. Changes in the sun's direct point between the tropic of cancer and the tropic of Capricorn, determines the altitude of solar, direct impact on the amount of solar radiation in the region. In this paper, we use the method in the paper of Huang Meisheng[24], to calculate the sun's direct point on the 15th of each month.

$$\delta = 23°44' \times \sin(360° \times \frac{284 + n}{365}) \tag{1}$$

δ is Sun declination, n is the number of days since New Year's Day.

The sun declination on the 15th of each month in 2014 as shown in **Table 2**

Table 2. Sun declination of monthly 15th.

Month	Sun declination	latitude axis of symmetry in level 1
1	21.5°S	18.3°S
2	10.1°S	13.56°S
3	2.9°S	4.56°S
4	9.5°N	2.69°N
5	19°N	12.9°N
6	21.6°N	17.38°N
7	21.8°N	16.38°N
8	14°N	7.5°N
9	2.3°N	1.88°N
10	9.6°S	2°N
11	19.3°S	7.31°S
12	23.6°S	15.8°S

Select a latitude randomly, to acquire the average value of SO_2 in the region, and make a straight line quadratic fitting to the sun's direct point corresponding. the results are shown in **Figure 1**.

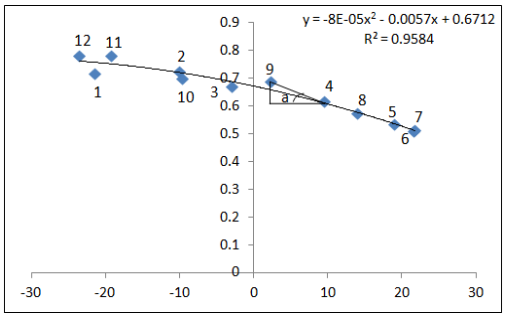

Note 1: In the figure, a is the tangent angle of the quadratic equation at the sun's point of incidence of 9.5 ° N

Note 2: 1,2, ..., 11,12 for the month

Figure 1. Fitting chart between SO_2 value and sun declination.

Find the derivative of the fitted equation f'(x), which is the derivative of the corresponding solar declination on the 15th of each month. In Fig. 1, April is known data and September is unknown. We use the regional data of April to calculate the unknown data of September. According to the definition of the function derivative, f (9) = f (4) -f ' (4)× [x (4) -x (9)]. Since the monthly spatial distribution of SO_2 in the same latitude shows latitudinal zonality, we assume that all the grids in the zonation satisfy the fitting equation and adopt the method of piecewise approximation. Similarly, we use September data to supplement March data to such a push, to supplement the missing month data in the band.

3. Results and Analysis

3.1. SO_2 columns in the same latitude

Method 1: The value of SO_2 at the same latitude is the same or similar, this is the premise of data

ISSN: 2424-8460(O)
2251-2608(P)

supplement. As shown in Fig. 2, the distribution of SO_2 at the same latitude extracted from the latitude of 48.15 ° N, as is showing that the distribution of SO_2 is more concentrated, and shows a certain movement integrally in the year.

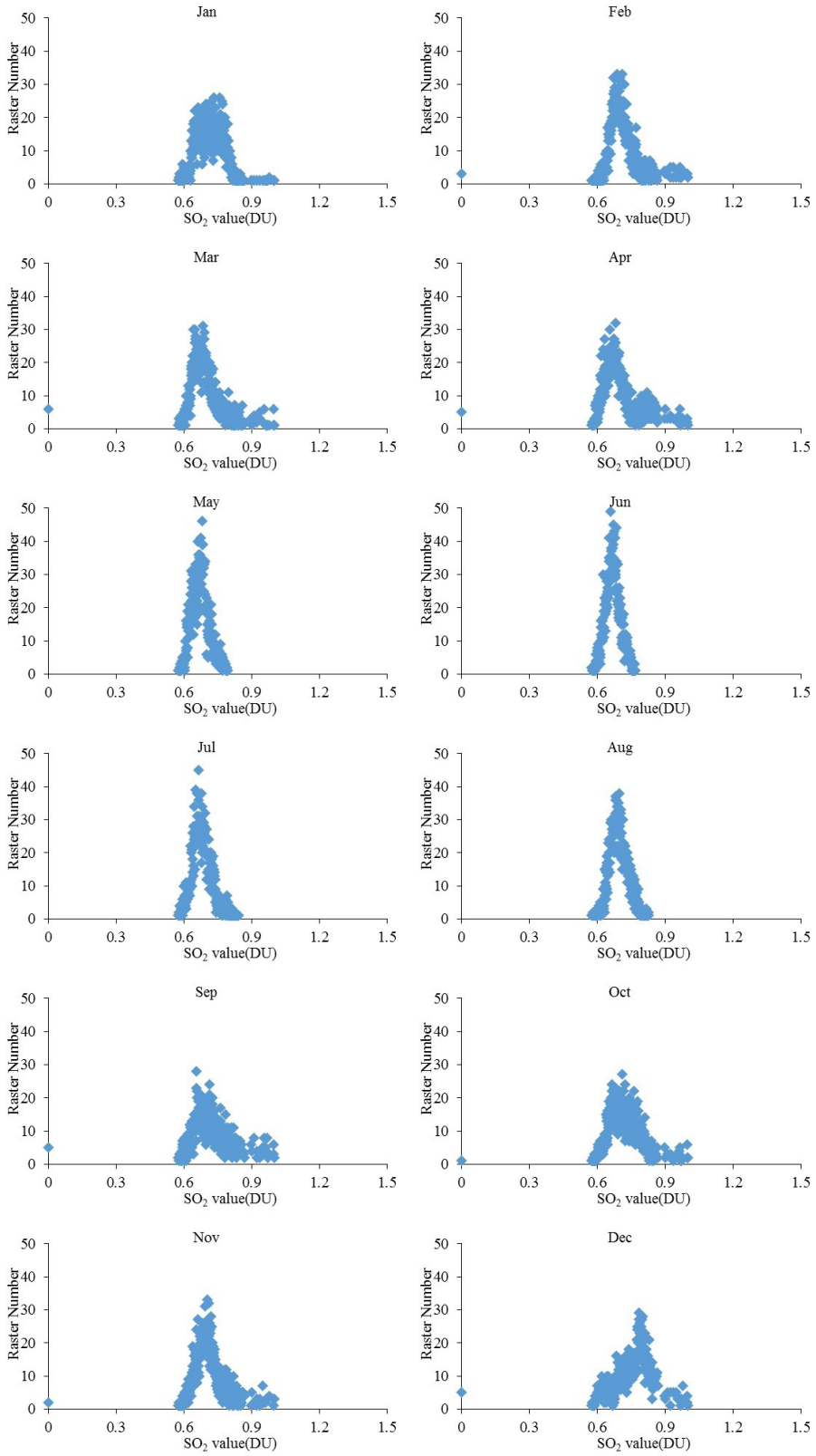

Figure 2. SO_2 value interval distribution at 48.15 ° N.

As shown in **Figure 2**, monthly SO_2 values were mainly distributed between 0.6DU and 0.8DU in January, February, March, September, and October. In April, SO_2 values were evenly distributed between 0.4DU- 0.599DU and 0.6-0.8DU respectively, accounting for 41.92% and 55.96% of the total grids respectively. From May to August, SO_2 values mainly ranged between 0.4DU and 0.599DU. In November and December, SO_2 values were evenly distributed between 0.6DU-0.8DU and 0.801DU-1.2DU, and the distribution of the two intervals was basically the same, showing good holistic characteristics. As the area is selected from the northern hemisphere, advance and retreat of the winter monsoon or the summer monsoon have a huge impact on the change of SO_2 values. In December, the winter monsoon became the strongest, and SO_2 concentrations mainly concentrated between 0.6-0.8DU and 0.801-1.2DU, with the decline of the winter monsoon, heating stopped and SO_2 values gradually decreased. In April, between 0.4-0.599DU and 0.6-0.8DU. When the summer monsoon approached, the values of SO_2 is further reducing and reaches to the minimum in June and July, mainly concentrated at 0.4-0.599DU, with the summer monsoon decline, it comes back to 0.6-0.8DU and 0.801-1.2DU, forming a cycle. The spatial distribution of monthly SO_2 at 10 ° N was also tried. The distribution results are similar to those at 48.15 °. SO_2 values concentration mainly concentrates in 0.3DU-0.5DU. Overall, the distribution of SO_2 concentration in the same latitude area is more similar, the trend of change is obviously the same.

Table 3. Distribution of SO_2 in 48.15 ° N.

Month	0.4DU-0.599 DU	0.6 DU-0.8 DU	0.801 DU-1.2 DU
January	1.21	92.67	6.11
February	1.77	87.11	12.43
March	13.23	78.98	7.82
April	41.92	55.96	2.12
May	93.36	6.63	0
June	99.65	0.35	0
July	94.58	5.41	0
August	76.38	23.62	0
September	12.61	73.53	13.85
October	2.92	88.75	8.33
November	0	63.56	36.44
December	0.24	54.78	45

Method 2: Select four cities around 53°N(Edmonton in Canada, Dublin in Ireland, Lipetsk and Chita in Russia) and three cities around 33°N(Phoenix in the United States, Djelfa in Algeria, and Xi'an in China).

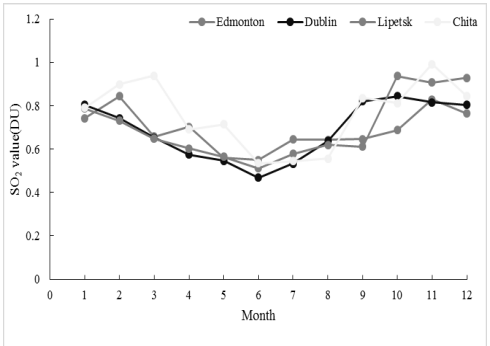

(a) Annual SO_2 change between four cities around 53°N

Figure 3. *(continued)*

ISSN: 2424-8460(O)
2251-2608(P)

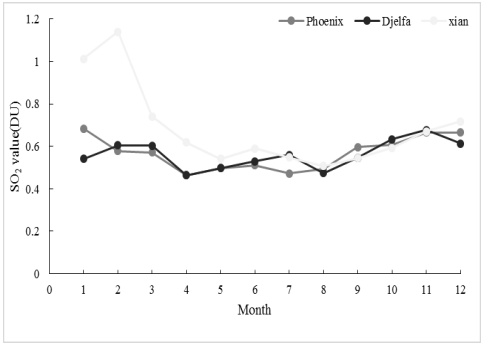

(b) Annual SO_2 change between three cities around 33°N

Figure 3. The second method to verify the annual change of SO_2 value at same latitude city.

As shown in Fig. 3, although the cities taken are located at different longitudes, different locations of land and different types of climate, the general trend of annual variation of SO_2 in atmospheric boundary layer basically remains the same during the year, showing a parabolic trend during the year, All SO_2 columns is basically the same.

In summary, the distribution of SO_2 column at the same latitude is more concentrated, the trend of change is obvious similar during the year, with Xi'an an exception mainly influenced by its terrain. This study mainly considers the temperature's influence on SO_2 in order to do some works about SO_2 distributions in the world.

3.2. Spatial distribution of OMI SO_2 data

OMI sensors use push-beam hyper-spectral imaging technology to detect the composition and magnitude of trace gases in the atmosphere by backscattered solar radiation in the ultraviolet to visible wavelength range. SO_2 products use two UV bands of 310.8-314.4nm and 345-370nm. The SO_2 in the atmosphere has a strong absorption effect on the electromagnetic waves in these two bands. The absorption causes the radiation energy to be converted into the intramolecular energy, thus causing the Two-band solar radiation intensity attenuation. Due to the Earth's revolution and rotation, when OMI sensors transit, there is no solar radiation in some areas, so the corresponding spectral information cannot be collected, resulting in difficulties in studying the spatial distribution of SO_2 in these areas or in a large area around the world. The range of SO_2 data in global at each month as shown in **Figure 4**.

The integrity area of OMI SO_2 data mainly concentrates in the area of 50 ° N-45 ° S, and the data of Northern Hemisphere high-latitude are lacking in winter, especially in the Arctic. The data of SO_2 are complete only in June and July; in the southern hemisphere, on the contrary, the data are relatively complete in November, December and January, the main shortcomings are in May, June, July, and August.

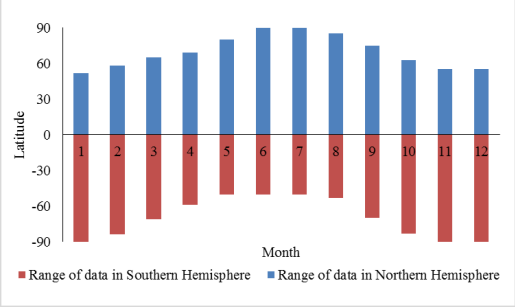

Figure 4. The global SO_2 data area changes with the month.

In this paper, Dimensional difference in the 5 ° zoning of 45 ° N-50 ° N and the 3 ° zoning of 47 ° N-50 ° N are selected in the region where data are complete, and the missing data are supplemented by the data of June, July, and August and make a verification of the accuracy, while verifying the dimensional difference influenced on its accuracy.

Table 4. Evaluating the results of the valuation from January to December at 45 ° N-50 ° N.

Range	Percentage of total area								
	Jan	Feb	Mar	Apr	May	Sept	Oct	Nov	Dec
<-1.5	0	0	0	0	0	0	0	0	0
[-1.5, -0.8)	0	0	0	0	0	0	0	0	0
[-0.8, -0.5)	0	0.11	0	0	0	0.34	0.24	0	0
[-0.5, -0.2)	0.12	1.1	1.93	2.53	0	12.83	5	0.4	0.37
[-0.2, 0)	11.63	29.41	27.42	41.11	52.84	72.31	51.6	45.8	47.14
[0, 0.2]	84.63	68.76	70.04	56.26	46.79	14.34	42.7	52.87	50.88
(0.2, 0.5]	3.62	0.61	0.62	0.1	0.37	0.18	0.46	0.93	1.61
(0.5, 0.8]	0	0	0	0	0	0	0	0	0
(0.8, 1.5]	0	0	0	0	0	0	0	0	0

Table 5. Evaluating results of the valuation from January to December in 47 ° N-50 ° N.

Range	Percentage of total area								
	Jan	Feb	Mar	Apr	May	Sept	Oct	Nov	Dec
<-1.5	0	0	0	0	0	0	0	0	0
[-1.5, -0.8)	0	0	0	0	0	0	0	0	0
[-0.8, -0.5)	0	0	0	0	0	0.5	0	0	0
[-0.5, -0.2)	0	0.	0	0	0	6.1	0.7	0.5	0.6
[-0.2, 0)	0.3	0.8	1.7	2.9	56.4	53.5	36.1	61.9	55.1
[0, 0.2]	18.3	35	27	47	42.9	39.3	61.4	36.8	42.6
(0.2, 0.5]	79.2	62.4	70.3	50.1	0.7	0.6	1.8	0.8	1.4
(0.5, 0.8]	2.2	1.8	1	0	0	0	0	0	0.3
(0.8, 1.5]	0	0	0	0	0	0	0	0	0

From the two sets of tables above, it can be seen that there is no substantial difference in the monthly SO_2 assessment, for the partition at 3° and 5°. The difference between the estimation and the actual monthly average SO_2 mainly concentrated in the range of -0.2DU ~ 0.2DU, which was lower than the monthly mean of SO_2 value of OMI, and the fitting evaluation was excellent, between -0.5 ~-0.2DU and 0.2DU ~ 0.5DU, which is lower than the standard deviation of PCA-retrieved background SO_2, which is ~0.5DU in the range of 30°N~30°S, the fitting evaluation is good; very few are in the range of -0.8DU ~ -0.5DU, ~0.8DU is the standard deviation of the range out 30°. Overall, this method works well for the complement.

A quadratic equation fitting and verification in regions which data are incomplete, starting from 55 °N, the missing data in northern hemisphere increases with latitude, and its loss are more in 85 °N ~ 90 °N with only 2 months complete. Co-deviation increases are large enough so that the supplementary results are poor and cannot accurately reflect the real data directly. In this study, the average data in the complete region close to regions where data are missing, are used to estimate the missing ones, an average by differences which are made by corresponding month except the lost ones, then averages are used to calculate the average value of the grid in the region where data are missing. Construct a quadratic equation with the existing data and the latitude of solar

declination on 15th every month. After the replenishment, the new quadratic equation is fitted again with the solar declination. We could made a function from the second fitting, by which the derivative f' (x) is also obtained. With the corresponding derivative values , sun Declination Department on the 15th of each month, and complete data in the region we could estimate the missing raster data, In this paper the girds of 55°N ~ 58°N are estimated by the data of 53°N ~ 55°N,and the accuracy is accessed at last.

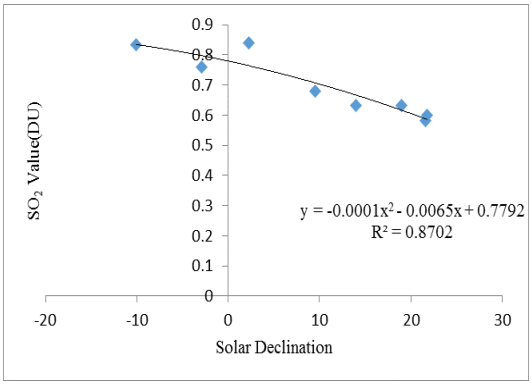

(a)

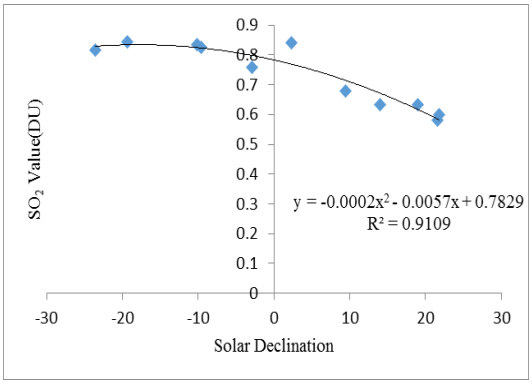

(b)

Figure 5. Fitting a quadratic equation with SO_2 and the latitude of solar declination on 15th every month.

In the regions of 53°N ~ 55°N, data from February to December are available, and in range of 55°N ~ 58°N, as is shown in **Figure 5-(a)**, available data are from February to September. Fitting from calculations and the remain ones, such as **Figure 5-(b)**, R^2 comes from the second's fitting is bigger than the first's, this means the fitting results are better as added data from the calculation. But slopes are decreased a little because of the data are added in, as is shown in **Table 8**, this means the calculated ones reaches the fitting line more closely.

The difference is made by the average of existing data at 53 ° N ~ 55 ° N and data of 55 ° N ~ 58 ° N correspondingly in the year, example in March, April, and September, estimate the missing data in that month, and re-fitting equation in 55 ° N ~ 58 ° N , supplement average SO_2 value in March, April, September, and then differences are made between the estimated value and the true value to evaluate the accuracy, as shown in **Figure 5-a**, **5-b**, In the area of the Americas and the Atlantic Ocean with the lower the value of SO_2, the estimations are overestimated by 0.2DU ~ 0.5DU, while SO_2 values in the middle and east Asia are underestimated by 0DU ~ 0.2DU, with excellent valuation accounting for 98.99% and 99.7% in March and April. Suffered by erupting of the Bardarbunga volcano on the September 14th, in southeastern Iceland, caused a substantial increase of SO_2 in parts of central Europe and Asia, severe under-estimation of SO_2 values in the Atlantic, Europe and parts of

central and western Asia, with the highest underestimation of 3.5DU. The difference accounted for 79.35%, in the range of (-0.5DU, 0.5DU) in September, which was nearly 20% lower than that in March and April. Therefore, this method is applicable in the range where there is no sudden change in the value of SO_2.

Table 6. Slope comparison.

Month	Sun declination	Slope come from existing data	Slope come from estimating data
Jan	-21.5°	-0.0012	-0.0012
Feb	-10.1°	-0.00448	-0.00348
Mar	-2.9°	-0.00592	-0.00492
Apr	9.5°	-0.0084	-0.0074
May	19°	-0.0103	-0.0093
June	21.6°	-0.01082	-0.00982
July	21.8°	-0.01086	-0.00986
Aug	14°	-0.0093	-0.0083
Sep	2.3°	-0.00696	-0.00596
Oct	-9.6°	-0.00458	-0.00358
Nov	-19.3°	-0.00264	-0.00164
Dec	-23.6°	-0.00178	-0.00078

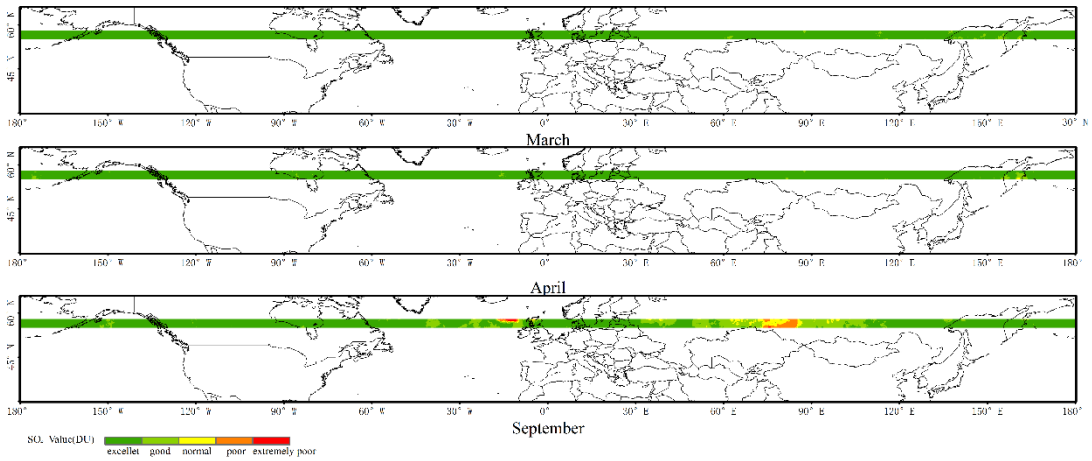

Figure 6. Evaluating estimated results in the region of 55°N~58°N.

3.3. Algorithm and verification

Within the 5 ° latitudinal zoning of 45 ° N-50 ° N, the monthly SO_2 data are complete for each month in the year. The grid average of the region is first fitted to the solar declination, then calculated monthly average SO_2 value in the missing month by the date of June, July, and August, and differences between the original and the calculating are computed, to evaluate the accuracy.

(1) Monthly average SO_2 columns in May: Based on the data of June as its' nearly than August, obtain SO_2 columns in May,

$$f(5) = f(6) - f'(5)[x(5) - x(6)] \quad (2)$$

(2) Monthly average SO_2 values in April: Based on the data in August, obtain the monthly average SO_2 in April,

$$f(4) = f(8) - f'(8)[x(8) - x(4)] \quad (3)$$

(3) Monthly average SO_2 volume in September: Based on the operational data in April, calculate the monthly average SO_2 in September,

$$f(9) = f(4) - f'(4)[x(4) - x(9)] \quad (4)$$

(4) Monthly average SO_2 value in March: Calculated on the basis of the operational data in September, and so on, to compute the SO_2 monthly averages in October, February, November, January, and December respectively. The results are shown in Fig7.

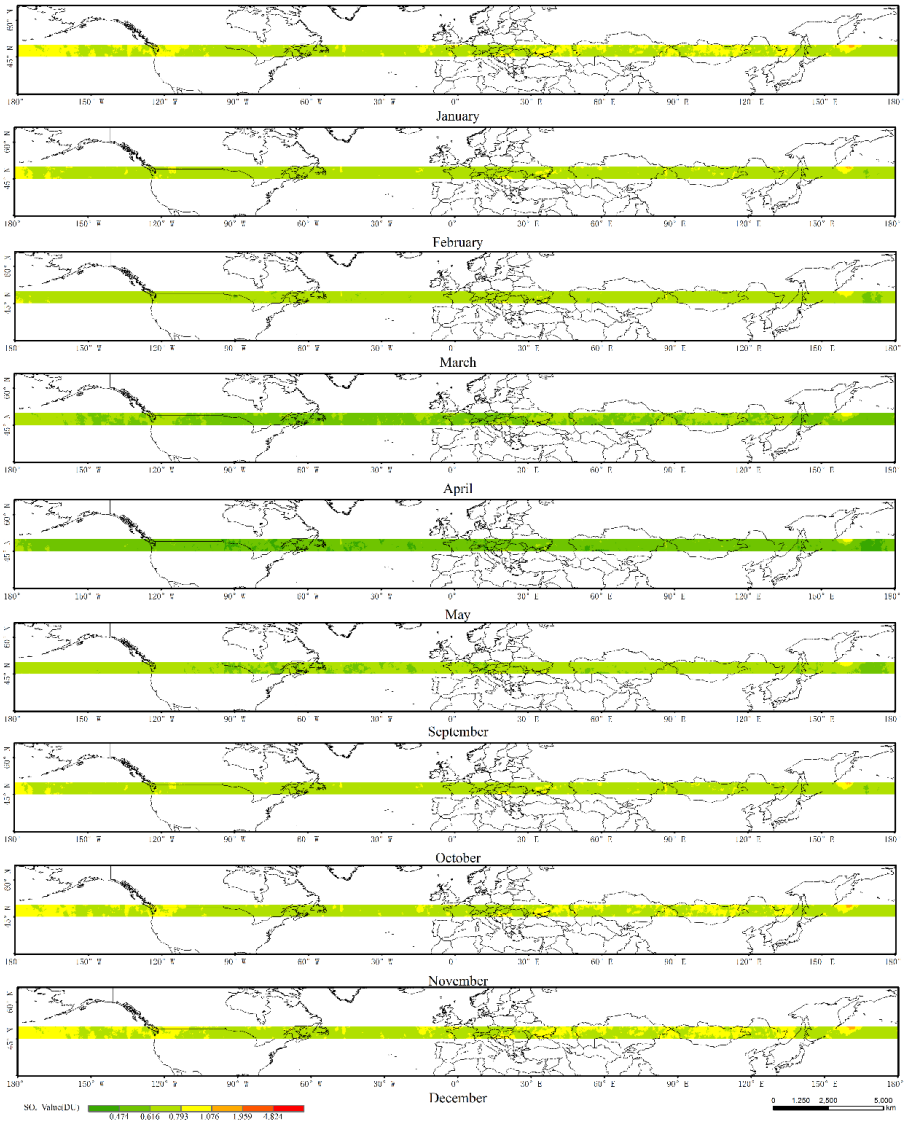

Figure 7. Results estimated in the region of 45°N~50°N.

As can be acquired from **Figure 7**, the monthly average SO_2 values are relatively concentrated except areas where emissions are high. The values are mainly concentrated in the range of 0.616DU ~ 0.793DU at January, February, March, September, October, November, and December in 45 ° N ~ 50 ° N, showing good latitudinal. In January, December and December, in the east and central Asia, Eastern Europe, the east coast of the Pacific and western North America, SO_2 values ranged from 0.793DU to 1.076DU, due to the winter heating and strong inversion layer, SO_2 increase, The values remain unchanged in other areas. In April and May With the increase

of temperature, the amount of SO_2 obviously decreased, and the decrease rate of the land area was obviously slower than the ocean, especially in the central and eastern Asia, and the decrease speed is slower.

In **Figure 8**, differences between the estimation and the actual is mainly concentrated in the range of [-0.2,0.2], there be more than 90% of estimated values are excellent. In September, affected by eruption of Bardarbunga, in southeastern Iceland, the difference is mainly concentrates in the range of [-0.5, -0.2) U (0.2,0.5], accounting for 3.74%, 1.72% and 2.54%, 2.63%, 0.37%, 13.35%,

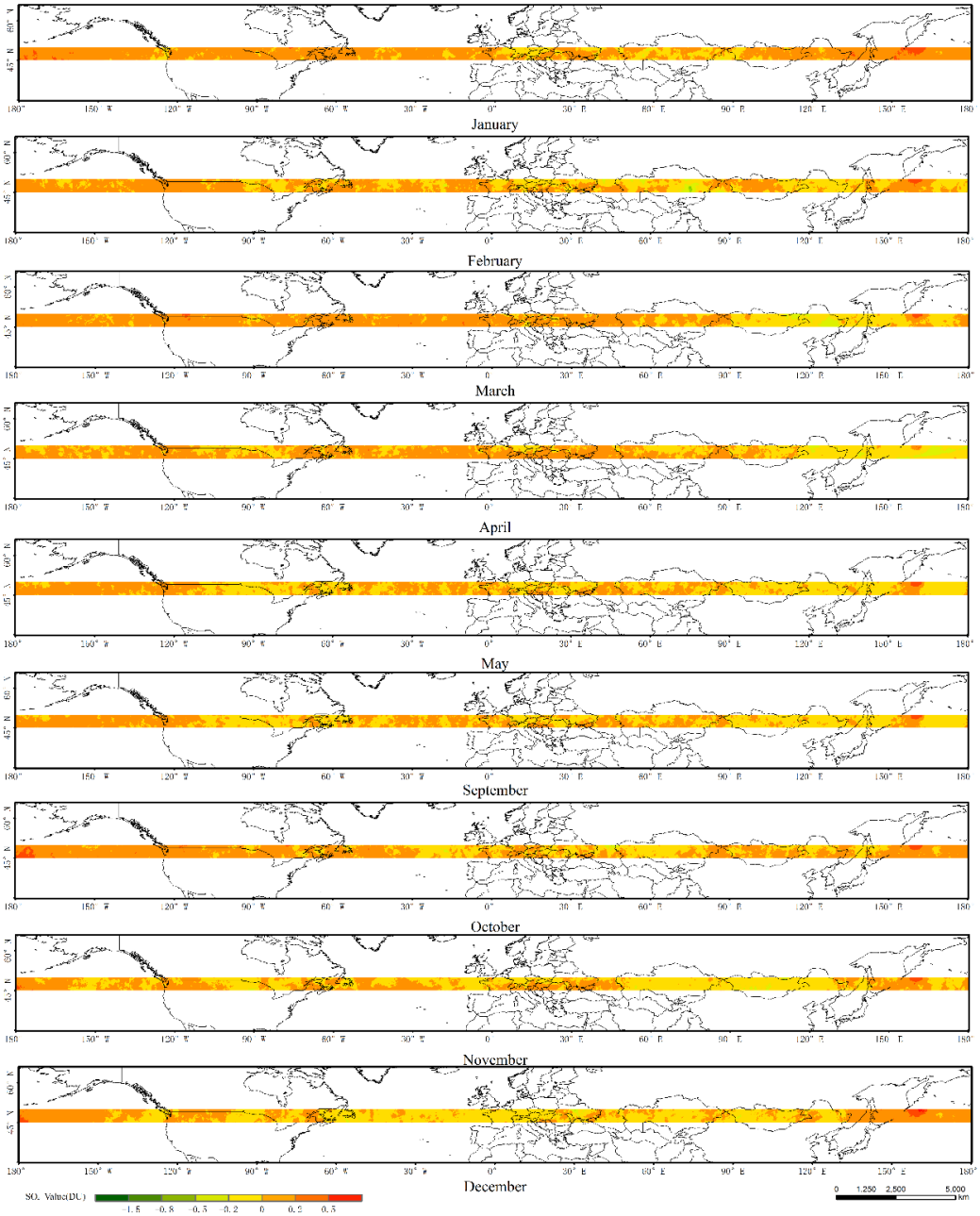

Figure 8. Evaluating results estimated in the region of 45°N~50°N.

5.46%, 1.33% and 1.91%, belongs to good valuation respectively. Evaluation of excellent and good is nearly close to the whole research area, so it is feasible to estimate the missing monthly average data by the method.

ISSN: 2424-8460(O)
2251-2608(P)

4. Global Spatial Distribution of PBL SO_2

Using the function derivative algorithm, the global OMI SO_2 data are supplemented. As shown in Fig.9, shows obvious zonal, the symmetrical distribution in the southern and northern hemispheres, and the aggregated distribution in regions where are the high emissions.

The of SO_2 columns are suddenly changed in the range of 75 ° N ~ 80 ° N over the area of 69 ° N ~ 75 ° N, caused by the eruption of the Bardarbunga volcano in September 2014, for a duration of up to 6 month (Gudmundsson M T et al.,2016), resulting in a significant increase of the SO_2 in Europe and Asia north of 69 ° N, but the data are missing from September at 75 ° N ~ 80 ° N, and the based data for the estimation is August, with no effect by erupting of the volcano, so the Regional SO_2 values were significantly underestimated, resulting in sudden changes in the area. In order to eliminate the impact of volcanic eruption in the range of 50 ° N ~ 75 ° N, this paper estimates the September's data based on April's, and then estimate the October, November, and December in 2014, as the result is shown in **Figure 10**,the influence, caused by volcanic eruption, can be filtered, meanwhile, regions can also be extracted by the method.

There is an SO_2 void over Antarctica at 70 ° S ~ 83 ° S, as is shown in Fig10. Under sunlight conditions, photochemical reactions occur between SO_2、O_3 and other gases (Huiming Zhang, 1998), resulting in a hole of SO_2 in Antarctica.

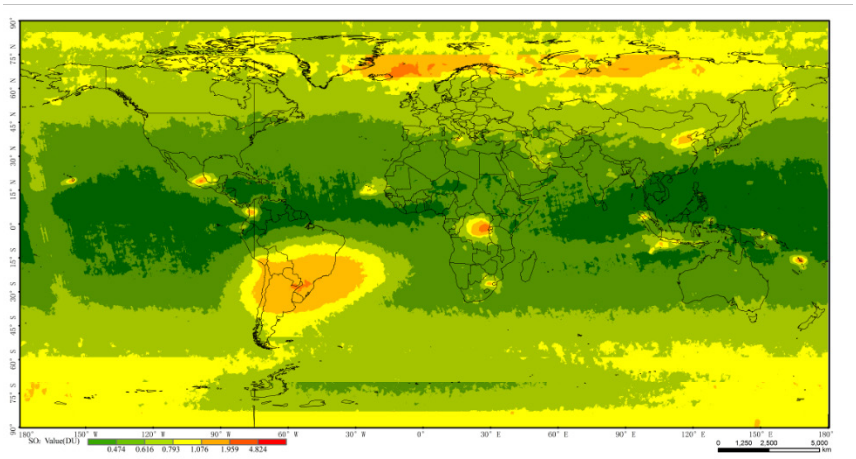

Figure 9. Global SO_2 spatial distribution.

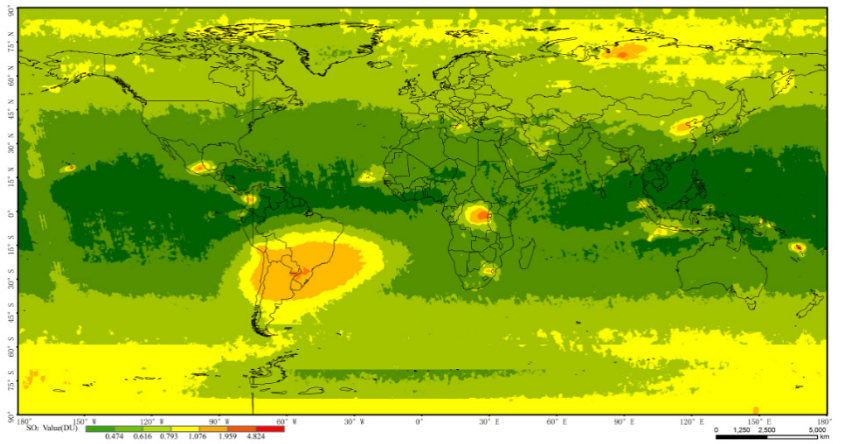

Figure 10. Global SO_2 spatial distribution after removing 65°N~75°N volcanic's influence.

5. Conclusion

In the course of studying the spatial distribution of SO_2 in the global atmospheric boundary layer by OMI SO_2, due to the limitation of the sensor itself, the revolution and the rotation of earth, SO_2 data cannot be collected as there is no sunshine. This paper attempts to supplement the global atmospheric boundary layer SO_2 by mathematical methods and the results show:

a)The global distribution of PBL SO_2 shows obvious latitudinal, columns and changing trends are same or similar. This is the precondition and foundation of this method. Through this feature, it is assumed that all the grids in the partition meet the fitting function equation.

b) latitude below 5 °, the zoning size has little influence in the accuracy of the estimation. If the technical conditions permit, the grid data can be fitted and estimated line by line, or for each raster;

c) In the area with none of the SO_2 data mutation, the function derivative algorithm can be suitable to supplement the global PBL SO_2 in segment approximation. By validating in the region of 45°N ~50°N, the data valuation is above 90% at-0.2D ~0.2DU, less than OMI SO_2 multi-day mean error;

d) In the areas with severe data loss, such as the northern frigid zone and the southern frigid zone, due to the small amount of monthly SO_2 data, resulting in the effect is not well, Complete missing data with the data nearby, corresponding monthly averaged, fitting, estimation and re-fitting methods to improve the accuracy of the supplementary. However, in the region where volcanic eruptions, caused SO_2 value mutation, the estimation results deviate significantly, The algorithm can be used to filter volcano's influence, and also can acquire the region where influenced by the eruption of volcanic.

In short, the function derivative algorithm, estimating and supplementing the global SO_2 value, achieving good results in most parts of the world, accurately reflecting the global SO_2 spatial distribution, providing technology for studying global SO_2 and climate change stand by.

References

[1] Zhang Y, Li C, Krotkov N A, J., 2017.Continuation of long-term global SO_2 pollution monitoring from OMI to OMPS. Atmospheric Measurement Techniques. 10(4),1-21. http://www.atmos-meas-tech.net/10/1495/2017/amt-10-1495-2017-supplement.pdf

[2] Robock A, J., 2000. Volcanic eruptions and climate. Reviews of Geophysics. 38(2),191–219. http://eos.ubc.ca/~mjelline/453website/eosc453/E_prints/1998RG000054.pdf

[3] Koike M, Kondo Y, Kita K, J., 2003.Export of anthropogenic reactive nitrogen and sulfur compounds from the East Asia region in spring. Journal of Geophysical Research Atmospheres. 108(20):1887-1902. http://onlinelibrary.wiley.com/doi/10.1029/2002JD003284.pdf

[4] Lee C, Richter A, Weber M, J., 2008.SO_2 Retrieval from SCIAMACHY using the Weighting Function DOAS (WFDOAS) Technique: comparison with Standard DOAS retrieval. Atmospheric Chemistry & Physics Discussions. 8(3), 6137-6145. https://www.cosis.net/members/meetings/abstracts/file.php/8/21445/jpdf/EAE03-J-08369.pdf

[5] Bell M L, Davis D L, J., 2001.Reassessment of the lethal London fog of 1952: novel indicators of acute and chronic consequences of acute exposure to air pollution. Environmental Health Perspectives Supplements.109 Suppl 3 (Suppl 3),389-394. http://120.52.51.19/europepmc.org/articles/PMC1240556/pdf/ehp109s-000389.pdf

[6] Lan Lan, D., 2013. Effects on Air Pollution on Public Health in Jinchang[D]. Lanzhou University. http://xueshu.baidu.com/usercenter/paper/show?paperid=2a21c570cbe216e9d5c5211411bc3719&site=xueshu_se

[7] Nyberg F, Gustavsson P, JRup L, J., 2000. Urban Air Pollution and Lung Cancer in Stockholm. Epidemiology 11(5),487-495. http://www.alarik.se/documents/LUCAS_Epidemiology2000nr11.pdf

[8] Yun Y , Gao R , Yue H , J., 2015. Synergistic effects of particulate matter (PM10) and SO_2 on human non-small cell lung cancer A549 via ROS-mediated NF-κB activation. Journal of Environmental Sciences, 31,146-153. http://or.nsfc.gov.cn/bitstream/00001903-5/199292/1/1000013192735.pdf

[9] Bovensmann H , Buchwitz M , Noel S, J., 2004.SCIAMACHY on ENVISAT: in-flight optical performance and first results. Proceedings of SPIE - The International Society for Optical Engineering, 5235,160-173. https://www.mendeley.com/catalogue/sciamachy-envisat-inflight-optical-performance-first-results/1198735.pdf

[10] Krotkov N A, Carn S A, Krueger A J, J., 2006. Band residual difference algorithm for retrieval of SO_2 from the aura ozone monitoring instrument (OMI). IEEE Transactions on Geoscience & Remote Sensing. 44(5),1259-1266. http://ieeexplore.ieee.org/stamp/stamp.jsp?tp=&arnumber=1624604.pdf

[11] Yang K, Dickerson R R, Carn S A, J., 2013.First observations of SO_2 from the satellite Suomi NPP OMPS: Widespread air pollution events over China. Geophysical Research Letters. 40(18),4957-4962. https://ntrs.nasa.gov/archive/nasa/casi.ntrs.nasa.gov/20140013038.pdf

[12] Carn, S. A, J., 2003. Prodigious sulfur dioxide emissions from Nyamuragira volcano, D.R. Congo. Geophysical Research Letters, 30(23),2211-2215. http://www.geo.mtu.edu/~gbluth/Publications/carn_2003_grl.pdf

[13] Khokhar M F, Frankenberg C, Roozendael M V, J., 2005. Satellite observations of atmospheric SO_2, from volcanic eruptions during the time-period of 1996–2002. Advances in Space Research. 36(5),879-887. http://citeseerx.ist.psu.edu/viewdoc/download;jsessionid=62BB5EB4B52A443C9467A00B81177723?doi=10.1.1.497.9333&rep=rep1&type=pdf

[14] Michael Eisinger, J., 1998. Tropospheric Sulfur Dioxide observed by the ERS-2 GOME Instrument. GEOPHYSICAL RESEARCH LETTERS. 25(22),4177-4180. http://doas-bremen.de/paper/grl_98_eisinger.pdf

[15] Fioletov V E, Mclinden C A, Krotkov N, J., 2011. Estimation of SO_2 emissions using OMI retrievals. GEOPHYSICAL RESEARCH LETTERS. 38,L21811. https://so2.gsfc.nasa.gov/pdfs/Fioletov_2011GL049402.pdf

[16] Krotkov N A, Mclinden C A, Li C, J., 2016. Aura OMI observations of regional SO_2 and NO_2 pollution changes from 2005 to 2015. Atmospheric Chemistry & Physics. 16(7),4605-4629. https://www.atmos-chem-phys-discuss.net/15/26555/2015/acp-2015-674-manuscript-version2.pdf

[17] Jiang J, D., 2012.Atmospheric SO_2 Concentration Monitoring and Emission Estimation in China Based on OMI Satellite Data and Numerical Simulations. Nanjing Normal University.

http://xueshu.baidu.com/usercenter/paper/show?paperid=21b2914213953202a590a59dbebb61a1&site=xueshu_se

[18] Xue D, Yin J, J., 2013.Meteorological influence on predicting surface SO_2 concentration from satellite remote sensing in Shanghai, China. Environmental Monitoring & Assessment, 186(5),2895. http://dx.doi.org/10.1007/s10661-013-3588-2.pdf

[19] Zhao Jun, Zhang Bincai, Fan Jieping, J., 2011. The Analysis of SO_2 value Changes in the Atmospheric Boundary Layer over Lanzhou and Surrounding Areas based on the OMI Product.Remote sensing Technology and Application. 26(6),808-813. http://xueshu.baidu.com/usercenter/paper/show?paperid=4d0f4d0d9f4587faf89cbf9def2a6516&site=xueshu_se

[20] Kang Chongyang, Zhao jun, Song guofu, J., 2018. Study on the spatial pattern of SO_2 in China's atmospheric boundary layer based on OMI data. CHINA ENVIRONMENTAL SCIENCECE. 38(2), 435-443. http://xueshu.baidu.com/usercenter/paper/show?paperid=bd50f4c9c66075e42b6ab2b94efd8f63&site=xueshu_se

[21] Wang Mingxing, Zhen Xunhua, M., 2005. Atmospheric Chemistry Introduction. Meteorological Press.

[22] Yang K, Krotkov N A, Krueger A J, J., 2007.Retrieval of large volcanic SO_2 s from the Aura Ozone Monitoring Instrument: Comparison and limitations. Journal of Geophysical Research Atmospheres, 112(D24),24-43. https://so2.gsfc.nasa.gov/pdfs/Yang_OMISO2_2007JD008825.pdf

[23] Li C, Joiner J, Krotkov N A, J., 2009. Retrieval of vertical columns of sulfur dioxide from SCIAMACHY and OMI: Air mass factor algorithm development, validation, and error analysis.114, D22303. http://www.iup.uni-bremen.de/doas/paper/jgr_09_lee.pdf

[24] Huang Meisheng, J., 1988.Use the formula to calculate the position of the sun and the latitude and longitude of the polar day and night. Middle School Geography Teaching Reference. (5),11-12. http://xueshu.baidu.com/usercenter/paper/show?paperid=013d8e417049f890ef80daefa781693b&site=xueshu_se